# Dose-dependent Mathematical modelling of Interferon-$\alpha$-treatment for personalized treatment of Myeloproliferative Neoplasms

Running head: Dose-dependent modelling of MPNs

Rasmus K. Pedersen[1,*], Morten Andersen[1], and Johnny T. Ottesen[1,*]

[1]Roskilde University, Roskilde, Denmark
[*]Corresponding Authors: rakrpe@ruc.dk and johnny@ruc.dk

For submission to *Computational and System Oncology*

Keywords: Mathematical Modelling, Personalized Treatment, Myeloproliferative Neoplasms, Interferon, (max: 7)
Title: 117 characters
Running head: 32 characters (max: 40)
Abstract word count: 279 words (max: 300)
Word count: Approximately 3400 (max: 3500)

# 1 Abstract

**Intro:** Long-term treatment with interferon-alfa (IFN) can reduce the disease burden of patients diagnosed with myeloproliferative neoplasms (MPN). Determining individual patient-responses to IFN-therapy may allow for efficient personalized treatment, reducing both drop out and disease burden.

**Methods:** A mathematical model describing hematopoietic stem cells and the immune system is suggested. Considering the bone marrow and the blood allows for modelling disease dynamics both in the absence and presence of treatment. Through comprehensive modelling of the effects of IFN, the model was related to individualized patient-data consisting of longitudinal hematologic and molecular measurements. Treatment-responses are modelled on a population-level, allowing for personalized predictions from a single pre-treatment data point.

**Results:** Personalized fits were found to agree well with data. This allowed for a quantitative description of the treatment-response, yielding a mechanistic interpretation of differences between individual patients. Population-level treatment-responses were simulated. Based on pre-treatment data and the actual treatment scheduling, the population-level response was found to predict the treatment-response of particular patients accurately over a five-year period.

**Conclusion:** Mechanism-based modelling of treatment effects demonstrates that hematologic and molecular observables can be predicted on the level of individual patients. Personalized patient-fits suggest that the effect of IFN-treatment can be quantified and interpreted through mathematical modelling, despite variation in hematologic and molecular response for different patients. Modelling suggests that both hematologic and molecular markers must be considered to avoid immediate relapse. Furthermore, personalized model-fits provides quantitative measures of the hematologic and molecular response, determining when treatment-cessation is appropriate. Proof-of-concept population-level modelling of treatment-responses from pre-treatment data successfully predicted clinical measures for a five-year period. This approach could have direct clinical relevance, offering expert guidance for clinical decisions about IFN-treatment of MPN-patients.

# 2 Introduction

The Philadelphia-negative myeloproliferative neoplasms (MPNs) is a group of blood cancers, which includes the diseases essential thrombocythemia (ET), polycythmia vera (PV) and primary myelofibrosis (PMF). MPNs progress slowly over several years, with severe side effects, such as an increased risk of experiencing dehabilitating thrombosis, and leukemic transformation where the patient acquires a secondary cancer, such as acute myeloid leukemia (AML) [5]. Chronic inflammation observed for MPN-diagnosed patients suggests that disease-progression and co-morbidity is driven by the immune system [13, 14]. Improved understanding of the link between disease progression and the immune system could improve future treatment by halting the disease before the cycle of chronic inflammation becomes uncontrollable. Therapy with pegylated Interferon-alpha (IFN) was investigated thoroughly in a recent clinical trial, showing that IFN causes an exponential decline in disease burden for long-term therapy [25]. Despite well-documented effects of IFN [20], and a history of IFN-therapy for MPN-patients [30] IFN is currently not a part of standard-of-care for MPN-patients everywhere.

Mathematical modelling of hematologic diseases has a long history [18, 7], with important medical advances and findings [9, 33, 32, 31, 34, 12, 19, 16, 15, 23, 1, 22, 21].

While validation and testing of predictive power of mathematical modelling is necessary before clinical application [4], mathematical modelling is apt to become an important part of clinical assessment of disease-stage and treatment, for both blood-cancers and localized tumours [8].

Mathematical models of hematopoietic stem cells (HSC) have given important insight about the hematopoietic system [17, 11, 3, 6, 26, 27]. Hematologic disease can arise from a malignant stem cell clone, leading many authors to explicitly model the malignant clone and the competition of stem cells [28, 2, 33]. Importantly, modelling suggests that treatment of HSC-derived disease must target the malignant stem cells [10, 1, 22, 21]. Consequently, mathematical models of hematologic malignancies should consider some notion of HSC if successful therapy is expected to be captured by model behaviour.

In a recent study, we mathematically modelled the IFN-induced decline in disease burden observed in MPN-patients, predicting whether a state of minimal residual disease would be attained [21]. The model described HSC, blood-cell production and immune-system feedback, and was originally calibrated to data from MPN-patients [1].

In this work, we propose a related model in which the description of HSC-behaviour has been expanded. The proposed model is related to both hematologic and molecular measures, demonstrating that both cell-counts and disease burden of MPN-patients can be modelled simultaneously. We first describe the model and how IFN-therapy was interpreted mathematically. A fitting-procedure relating the model to data of individual patients is described. Personalized modelling suggests that molecular measures are necessary to determine treatment-cessation will cause an early relapse. Population-level model predictions are made for a sub-cohort of patients,

in which the full period of IFN-treatment (up to five years) is predicted from a single pre-treatment data-point. This proof-of-concept result suggests that mathematical modelling on both individual- and population-level could be a useful clinical tool in the near future, predicting e.g. the outcome of treatment-cessation or increases in dosage.

# 3 Materials and Methods

## 3.1 Mechanism-based mathematical model of the hematopoietic system

To model the effect of IFN on the MPN patients of the DALIAH trial described above, we first introduce a mathematical model of the healthy hematopoietic stem cells (HSC), leukemic stem cells (LSC), blood cells and the immune cells. The model is based on two previously presented models: The Cancitis model [1, 21] and a model of HSC-dynamics within the bone marrow [27].

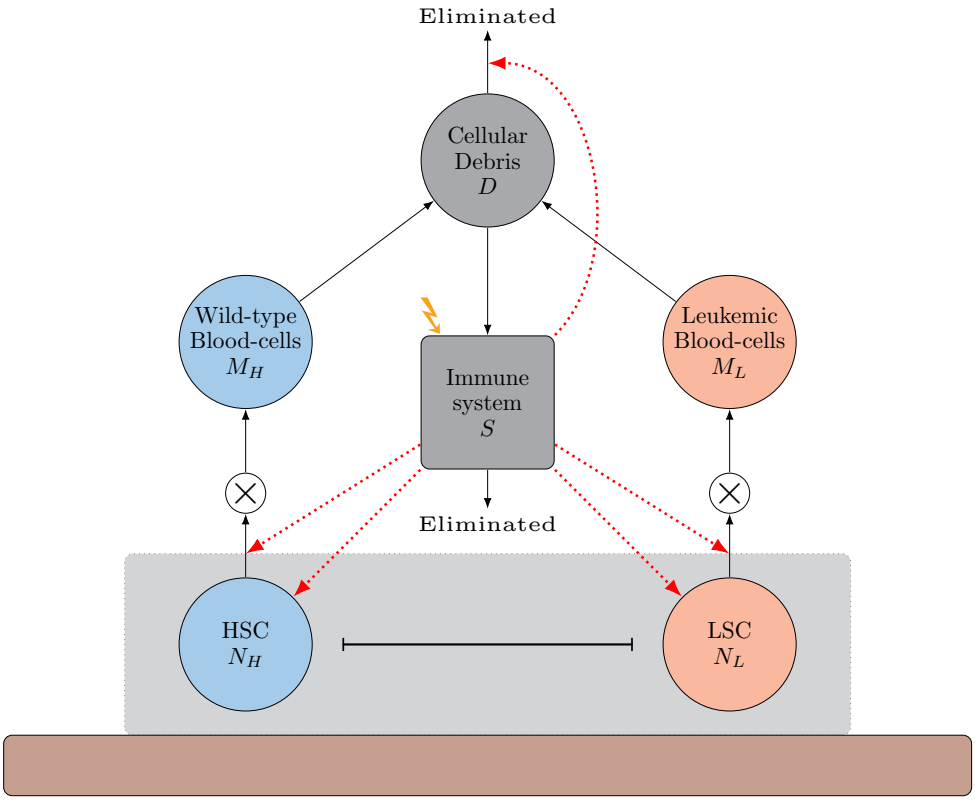


Figure 1: **Schematic compartment diagram of mathematical model** Wild-type HSC and the produced blood-cells, $N_H$ and $M_H$ respectively, are shown as blue circle on the left, while LSC and the LSC-derived blood-cells, $N_L$ and $M_L$ respectively, are shown as red circles on the right. The cellular debris arising from natural cell-death of blood-cells, $D$, is shown as a grey circle, while the immune system, $S$, is represented by a grey box in the middle. Black arrows represents flows between compartments, and red arrows signify upregulation by the immune system. The circle with $\times$ represent a multiplication in numbers to the proliferation of progenitor-cells. The self-renewal of HSC and LSC is not depicted in the figure due to its non-linear form, however the grey box and the line connecting HSC and LSC represented this interaction of stem cells within the bone-marrow niches (shown as a dark-red box at the bottom).

The model is given by a system of ordinary differential equations describing the amount of wild-type HSC $N_H$, the amount of LSC $N_L$, the number of mature blood-cells arising from the wild-type HSC $M_H$, the number of mature blood-cells arising from the LSC $M_L$, the amount of cellular debris $D$, and an abstract measure of the immune system response, $S$. The stem-cell dynamics of the model of Pedersen et al. [27] give rise to a production of blood-cells. Following apoptosis (programmed cell-death) the cell-debris ($D$) upregulates the immune system ($S$), which increases stem-cell production, to maintain cell-counts. This ensures a robust hematopoietic system, that can model both disease-free hematopoeisis, early-disease stages and treatment. A schematic diagram of

the model is shown in figure 1. Additional details about the model-formulation is given in the supplementary material. The model is given as the following system of ordinary differential equations, describing the gain and loss of each of the six variables:

$$\dot{N}_H = \mu_H S \left( \frac{2\gamma\rho_H (1 - N_H - N_L)}{\alpha_H + 1 - N_H - N_L} - 1 \right) N_H \tag{1a}$$

$$\dot{N}_L = \mu_L S \left( \frac{2\gamma\rho_L (1 - N_H - N_L)}{\alpha_L + 1 - N_H - N_L} - 1 \right) N_L \tag{1b}$$

$$\dot{M}_H = \omega_H \kappa_H S - d_H M_H \tag{1c}$$

$$\dot{M}_L = \omega_L \kappa_L S - d_L M_L \tag{1d}$$

$$\dot{D} = d_H M_H + d_L M_L - e_D D S \tag{1e}$$

$$\dot{S} = r_S D - e_S S + g \tag{1f}$$

where $\kappa_j = \left( 2 - 2\rho_j + \frac{2\gamma\alpha_j\rho_j}{\alpha_j + 1 - N_H - N_L} \right) \mu_j \Theta N_j$. All parameters are non-negative. Additionally, $\rho_j \leq 1$ and $\gamma \geq 1$. Default values given in table 1, along with a brief description of what biological processes the parameters represent. It can be shown that all variables remain non-negative for non-negative initial conditions. A numerical solution representing a typical disease-progression scenario is depicted in figure 2, together with simulated treatment, as described in section 3.2.

We define the disease level in the model as the relative frequency of blood-cells derived from LSC out of all blood-cells, $\frac{M_L}{M_H + M_L}$.

A fraction of the total blood-cell count in the model is assumed to be of a particular cell-type. We define the thrombocyte-count as $C_{thro} = R_{thro}(M_H + M_L)$ and the leukocyte-count as $C_{leuk} = R_{leuk}(M_H + M_L)$, where $R_{thro}$ and $R_{leuk}$ are the cell-specific fractions.

Mathematical analysis of the model was described in [24]. We omit a thorough mathematical analysis here, however some brief comments are warranted. For most choices of model-parameters, three steady states exists: A trivial steady state with no cells, a healthy steady state with $N_L = M_L = 0$ and a full-blown leukemic steady state with $N_H = M_H = 0$. Numerical investigations of local stability reveals that typically only one steady state is stable, while the two others are unstable. This suggests that for a given choice of parameters, the system will asymptotically approach the stable steady state. This allows us to compute the long-term effect of treatment. To investigate the transient behaviour during treatment, the model can be solved numerically, simulating particular treatment-effects on parameters.

## 3.2 Modelling treatment-effects

Treatment with IFN has been found to deplete the population of LSC that give rise to MPN [20]. To model this effect, we consider an IFN-induced decrease of $\rho_L$, the parameter related to LSC differentiation. Preliminary model investigations revealed that decreasing $\rho_L$ resulted in depletion of LSC and a decrease in the disease level. Visual inspection of data suggests a transient effect of IFN on the total cell-count, reducing both healthy and leukemic mature cells before the disease level decreases. A change in the proliferation of both healthy and leukemic progenitor cells, as modelled by parameters $\omega_H$ and $\omega_L$ respectively, could explain such decrease in total cell count. Hence, when modelling IFN-treatment, we perturb parameters $\rho_L$, $\omega_H$ and $\omega_L$. To reduce the degrees of freedom, we consider only equal perturbation of $\omega_H$ and $\omega_L$, such that the relation $\omega_L = 2.5\omega_H$ is maintained throughout this work for both default parameter-values and perturbed parameters. Perturbation of $\rho_L$ affects primarily the relative frequency of cells while perturbation of $\omega_H$ and $\omega_L$ affects the total amount of mature blood cells. A numerical example of perturbing these parameters is shown in figure 2. Within the first year of treatment, a transient effect of perturbing $\omega_H$ and $\omega_L$ causes a pronounced decrease in blood-cell counts. A corresponding transient increase is seen when treatment is ceased. This transient effect occurs because $\omega_H$ and $\omega_L$ affects both healthy and leukemic blood-cells, and as a consequence, without perturbation of $\omega_H$ and $\omega_L$, the transient decrease of total blood-cells counts does not occur (not shown).

For default parameters, solutions of the model approach the full-blown leukemic steady state for any positive number of malignant stem cells, and hence, relapse always occurs. However, the degrees of parameter-perturbation considered in the simulated treatment affects the time until relapse occurs. To estimate the time between treatment-cessation and relapse, we defined a relapse-threshold of $1.5 \cdot 10^{12}$ blood-cells, corresponding to a 50% increase compared to the healthy steady state count. When total blood cell counts exceed this value after treatment-cessation, relapse is assumed to have occurred. For the example shown in figure 2, relapse occurs 6 years after treatment cessation, around year 28. Simulating a range of treatment-specific values of $\omega_L$, $\omega_H$ and $\rho_L$, we investigated the resulting time to relapse. The results are shown in figure 3. While changes

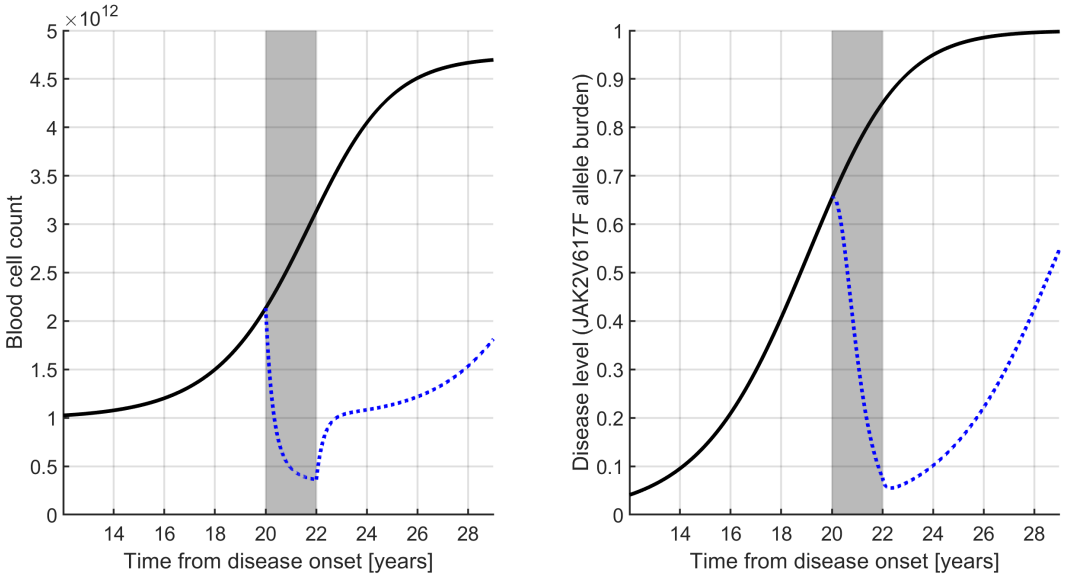


Figure 2: **Illustrative model simulation with treatment affecting $\rho_L$, $\omega_H$ and $\omega_L$.** Starting in the healthy steady state at time $t = 0$ (with $M_H \approx 1 \cdot 10^{12}$), one HSC is removed from $N_H$ and added to $N_L$. Due to the growth advantage of the leukemic clone for default parameters, the disease progresses in absence of treatment. This progression is shown in black in both panels. The relative frequency of malignant mature cells, $\frac{M_L}{M_H+M_L}$, reaches approximately 65% within 20 years. Between year 20 and 22 a treatment-scenario is simulated, setting $\rho_L = 0.515$, $\omega_H = 2 \cdot 10^6$ and $\omega_L = 5 \cdot 10^6$. At year 22, parameters are reset to their default values. The left panel depicts the mature cell-counts, $M_H + M_L$, with the dotted blue line depicting the simulated treatment-scenario. The right-hand panel shows the relative frequency of malignant mature cells, $\frac{M_L}{M_H+M_L}$, with the dotted blue curve showing the scenario with treatment. The grey background illustrates the treatment-period.

| Parameter | Value | Description | Parameter | Value | Description |
|---|---|---|---|---|---|
| $\mu_H$ | 0.0376 | Release-rate from bone-marrow niche, HSC | $\mu_L$ | 0.0432 | Release-rate from bone-marrow niche, LSC |
| $\rho_H$ | 0.5289 | Rate of self-renewing proliferation, HSC | $\rho_L$ | 0.5310 | Rate of self-renewing proliferation, LSC |
| $\alpha_H$ | 0.0053 | Post-cell-division differentiation-rate, HSC | $\alpha_L$ | 0.0051 | Post-cell-division differentiation-rate, HSC |
| $\Theta$ | 15000 | Number of quiescence-inducing stem cell niches within bone-marrow | $\gamma$ | 1 | Effective new daughter-cells per stem cell division |
| $\omega_H$ | $4.7 \cdot 10^6$ | Blood-cells produced per stem cell differentiation, HSC | $\omega_L$ | $11.75 \cdot 10^6$ | Blood-cells produced per stem cell differentiation, LSC |
| $d_{M_H}$ | 0.0129 | Death-rate, healthy mature cells | $d_{M_L}$ | 0.0129 | Death-rate, leukemic mature cells |
| $e_D$ | $2 \cdot 10^5$ | Clearance-rate of cellular debris | $r_S$ | 0.0003 | Debris-dependent immune-system activation |
| $e_S$ | 2 | Immune-system inactivation | $g$ | 7 | External inflammation |

Table 1: **Default parameters used in simulations.** Parameters $u_H$, $u_L$, $d_{M_H}$, $d_{M_L}$, $e_D$, $r_S$ and $e_S$ are in units of $[days^{-1}]$, while the other parameters are without unit. Parameters $u_L$, $\rho_L$, $\alpha_L$ and $\omega_L$ were determined from the healthy counterparts and were modified to agree with the disease progression as described in [25]. The remaining default values were determined in the work described in [21] and [26].

to $\omega_H$ and $\omega_L$ are important for a transient reduction in blood-cell counts, the effect on the time to relapse is minor. Conversely, reduction of $\rho_L$ lengthens the time to relapse.

### 3.3 Data

We consider data from the prospective randomized open-label phase III clinical trial "DALIAH" (EudraCT number: 2011-001919-31) [25, 21]. In the trial, a cohort of MPN-patients received Pegylated r-IFN$\alpha$ (IFN) monotherapy (Either Interferon alfa-2a "*Pegasys*" or Interferon alfa-2b "*PegIntron*"). Data consisted of IFN-dosage and timing, as well as longitudinal hematologic and molecular measurements. In particular, the thrombocyte- and leukocyte-counts as well as the $JAK2^{617F}$ (JAK2) allele burden were measured. We consider the JAK2 allele burden a measure of the disease progression. A total of 63 patients [21] are here considered, 17 of which were diagnosed with ET, 35 with PV, 6 with PMF and 5 patients with prefibrotic myelofibrosis.

### 3.4 Pharmaco-kinetic modelling of IFN-dose

IFN was given on a weekly, bi-weekly or tri-weekly basis, in a range of dosages. For simplicity, we here report a daily average dose. A pharmaco-kinetic (PK) model of IFN was considered, in agreement with our previous work [21]. We assume an equal rate of uptake and clearance of IFN, $\tau = \frac{1}{7}\frac{\mu g}{\text{day}}$, inspired by previous work on PK modelling of IFN [29]. Letting $I(t)$ denote the stepwise constant daily dose in units of $\mu g$ IFN, we choose the simplest possible PK description of the blood-concentration:

$$\dot{B}(t) = \tau(I(t) - B(t)) \tag{2}$$

where the dot denotes the time-derivative. The IFN blood-concentration $B(t)$ is in units of $\mu g$ IFN, assuming a constant blood volume and ignoring patient-specific variations in volume. For constant $I(t) = I_0$, administered

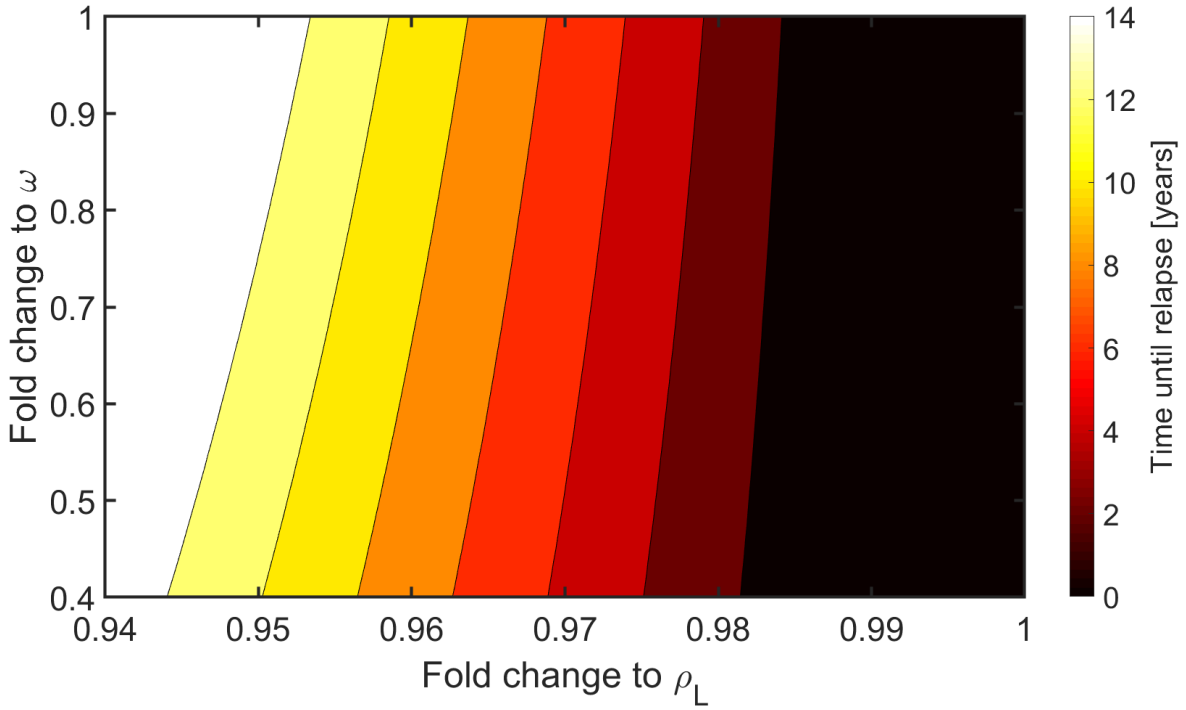


Figure 3: **The relationship between the modelled treatment response and time to relapse.** The scenario of figure 2 was simulated, with two years of simulated treatment from year 20 to year 22. A range of values of $\rho_L$, $\omega_H$ and $\omega_L$ during treatment was considered. The time from treatment cessation (at year 22) until total blood-cell counts exceeded $1.5 \cdot 10^{12}$ were determined. The vertical axis signifies the change of both $\omega_H$ and $\omega_L$, as the relation $\omega_L = 2.5\omega_H$ was maintained. The simulated scenario of figure 2 corresponded to a 0.97 fold change of $\rho_L$ and a 0.43 fold change to $\omega_L$ and $\omega_H$.

with onset at time $t = t_0$, this differential equation may be solved explicitly:

$$B(t) = I_0 - (I_0 - B(t_0))e^{-\tau(t-t_0)} \tag{3}$$

### 3.5 Pharmaco-dynamics of IFN

The pharmaco-dynamics (PD) of IFN is modelled such that parameter-perturbation depends directly on the blood-concentration of IFN. For the perturbation of $\omega_H$ and $\omega_L$, we define $\hat{\omega}_H$ and $\hat{\omega}_L$ as functions of the blood-concentration $B$:

$$\hat{\omega}(B) = \begin{cases} (1 + \nu_\omega B)\omega & \text{for } \nu_\omega \geq 0 \\ e^{\nu_\omega B}\omega & \text{for } \nu_\omega < 0 \end{cases} \tag{4}$$

where the parameter $\nu_\omega$ describes how significant the parameter is perturbed. For $\nu_\omega < 0$, the parameter is reduced, while it is increased for $\nu_\omega > 0$. For all values of $\nu_\omega$, $\hat{\omega} \geq 0$ is fulfilled.

A different perturbation for $\rho_L$ is considered, since $\rho_L \leq 1$ must be maintained for all doses. We define $\hat{\rho}_L$ as:

$$\hat{\rho}_L(B) = \frac{\rho_L}{\rho_L + (1 - \rho_L)e^{-\nu_{\rho_L} B}} \tag{5}$$

where $\nu_{\rho_L}$ determines the degree of response to treatment.

For the patients considered, the time-dependent blood-concentration, $B(t)$, was described in section 3.4. Hence, both $\hat{\omega}_H$, $\hat{\omega}_L$ and $\hat{\rho}_L$ are time-dependent.

### 3.6 Procedure for obtaining individualized patient-fits

Combining data for IFN-dose with the parameter-perturbations described by the PK- and PD-modelling described in sections 3.4 and 3.5, the response of an individual patient to IFN-treatment could be represented by two parameters, $\nu\rho_L$ and $\nu\omega$.

Three measures were considered for determining how well the model agreed with data; The disease-level error, defined as the sum of squared errors (SSE) between model disease-level and the JAK2 allele burden, the thrombocyte-error, defined as the SSE ofthe thrombocyte-counts and the (scaled) blood-cells counts and finally the leukocyte-error, defined as the SSE of leukocyte-counts and the (scaled) blood-cell counts.

For the 63 patients considered, personalized model-fits were determined. A model-simulation without treatment was shifted in time such that at $t = 0$ the model disease agreed with the baseline-measurement of the JAK2 allele burden of the patient. This could also be used to estimate the time of initial mutation and disease onset, see [25].

Subsequently, we used an iterative three-step data-fitting procedure. Initially, a value of $\nu\rho_L$ was found that minimized the disease-level error, using the `MATLAB` function `fminsearch`. Secondly, blood-cell scaling-factors $R_{thro}$ and $R_{leuk}$ and treatment-parameter $\nu\omega$ were fitted such that the thrombocyte-error and leukocyte-error were minimized. Finally, an additional optimization of $\nu\rho_L$ with the disease-level error was carried out, and scaling-factors $R_{thro}$ and $R_{leuk}$ were re-optimized to minimize thrombocyte-error and leukocyte-error.

We emphasize that the procedure priorities the agreement between the disease burden, as given by the JAK2 allele burden in data and model disease-level given by $\frac{M_L}{M_H+M_L}$, rather than cell-counts.

# 4 Results

## 4.1 Patient fits

Personalized values of $\nu_{\rho_L}$, $\nu_\omega$, $R_{trom}$ and $R_{leuk}$ were determined for each patient, describing the patient-specific response to IFN of the given patients. This was done for all 63 patients from the DALIAH trial. The resulting numerical solutions of the model are shown in the supplementary material, and two examples are shown in figure 4. In all figures, patient-ID's are used that correspond to those used in [21]. The model reproduces both the dynamics of hematologic measures (blood-cell counts) and molecular measures (the JAK2 allele burden), and was found to agree with both patients that respond well to treatment and patients that do not.

Good responders are characterized by a significant decrease in disease burden and a normalization of cell counts. As changes to $\rho_L$ primarily affects the disease burden while $\omega_H$ and $\omega_L$ affect the total cell count, the fitted values of $\nu_{\rho_L}$ and $\nu_\omega$ identifies good-responders. In particular, good responders are found to have fitted values lower than those of bad responders. Hence, the patient fits provide quantitative measures for how well a patient responded to treatment.

Patient-specific fits allows us to simulate hypothetical treatment-scenarios. In particular, we can consider the effect of halting treatment. In figure 5 two simulated scenarios are shown for a particular patient, halting treatment after 0.5 and 5 years. When treatment was ceased early, cell-counts rapidly return to elevated levels, with thrombocytes above the healthy interval within half a year. After five years of treatment, we find that approximately nine years without treatment is possible before the thrombocyte-count exceeds the threshold. Note that cell-counts at the times chosen were approximately equal (just below $300 \cdot 10^3$ cells per $\mu L$), both in the model and in data. Hence, the stage of disease at year 0.5 and year 5 would be indistinguishable, if based solely on cell-counts. Our findings suggests that monitoring the disease burden is important to determine the time to relapse.

## 4.2 Cell-counts at steady state

For all patients, scaling factors were found, relating the modelled sum of mature cells to the blood-cell counts observed in data. Scaling the steady state value of $M_H$ in the healthy steady state with the scaling-factor gives a patient-specific estimate of pre-disease cell-counts. For most patients, these cell-counts are found to be within the healthy interval, validating the model in the absence of disease. Scaling the steady-state value of $M_L$ in the full-blown leukemic steady state provides an estimate for the cell-count that would be approached if no treatment had been initiated. Significantly increased blood-cell counts were predicted at the leukemic steady state. As heightened blood-cell counts are a diagnostic criteria, this further validates the model in absence of treatment. Additional details along with histograms of the steady state values are given in the supplementary material.

## 4.3 Population modelling of patient response

While the model was found to agree well with most patients, the model reproduced data of a sub-cohort of 20 patients particularly well. These were not necessarily patients that respond well (or poorly) to treatment, but rather determined by particular selection criteria. Details are given in the supplementary material. Based on this sub-cohort, a two-dimensional log-normal distribution of $\nu_{\rho_L}$ and $\nu_\omega$ was determined. This distribution describes the treatment-response parameters on a population-level.

From the distribution, 1000 virtual patients were chosen, described by dose-dependent parameter-perturbations. For each of the virtual patients, we simulated treatment schedules identical to each of the 20 patients in the sub-cohort. For these simulations, initial conditions corresponding to those of the baseline measurement of the real patient were used. In figure 6, an example is shown.

We consider an entirely simulated patient-response. Mean baseline values of patients diagnosed with PV were leukocyte-counts of $11.4 \cdot 10^3(\mu L)^{-1}$, thrombocyte-count of $571 \cdot 10^3(\mu L)^{-1}$, and JAK2 allele burden of 44%. Simulating 1000 virtual patient responses with the mean baseline values as initial conditions and a daily dose of $5\mu g$ IFN (a weekly dose of $35\mu g$ IFN), we determined the expected distribution of patient-responses illustrating the treatment-response of an idealized PV patient. The results are shown in figure 7.

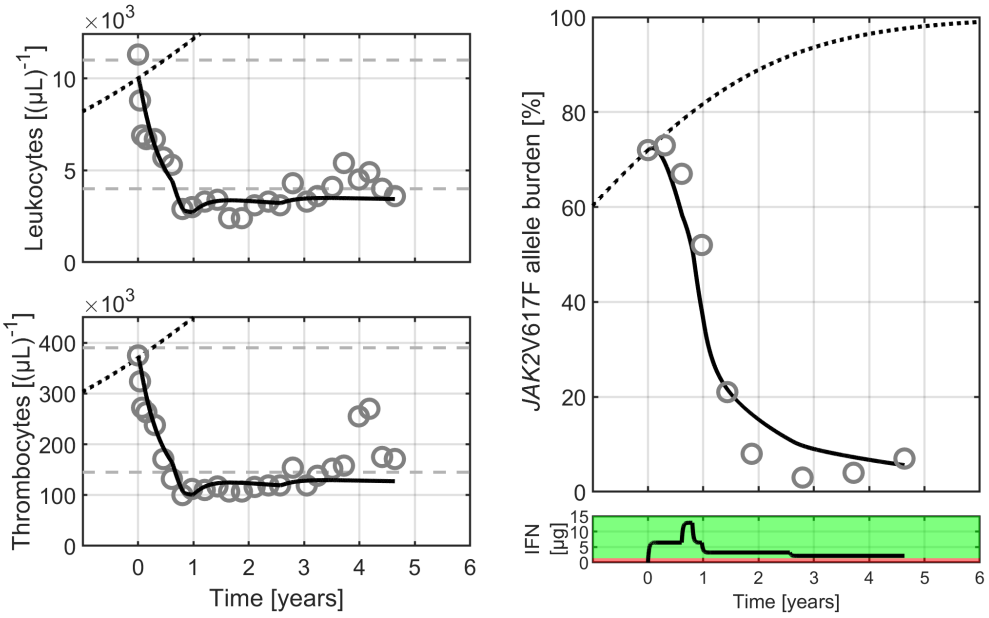


(a) Patient P082

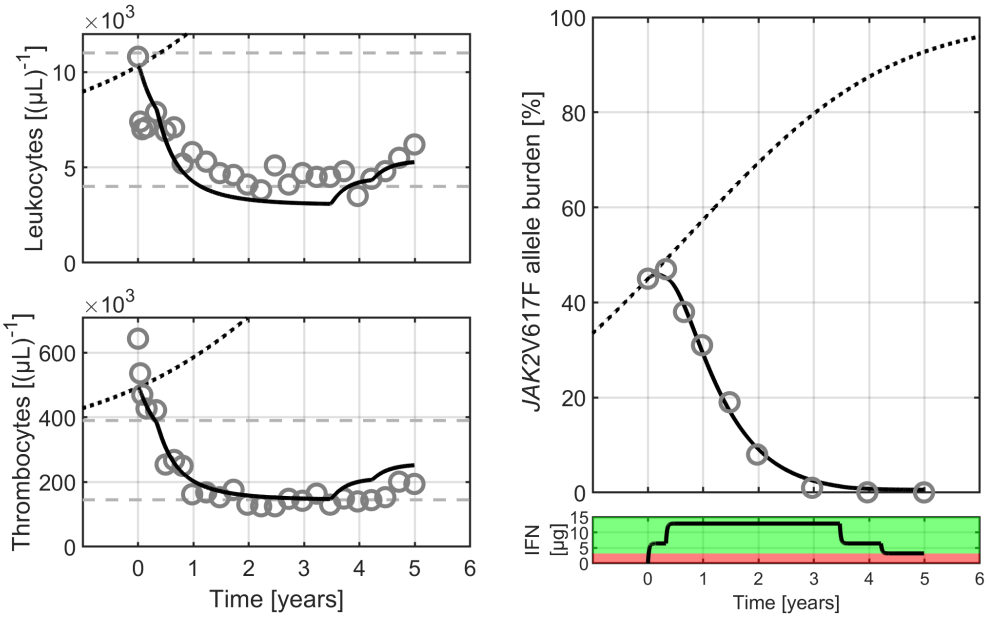


(b) Patient P198

Figure 4: **Examples of patient-specific fits of the model.** The left panels display the blood-cells count as grey circles. The black curve displays the sum of mature cells, $M_H + M_L$, scaled by the appropriate scaling factors. A simulation without treatment is shown dotted black for comparison. Approximate healthy intervals of cell-counts are shown in dashed grey, defined as between $145 \cdot 10^3$ and $390 \cdot 10^3$ thrombocytes per $\mu L$ and between $4 \cdot 10^3$ and $11 \cdot 10^3$ leukocytes per $\mu L$. In the right-hand panel, the model disease level is shown together with the JAK2 allele burden data. A treatment-free simulation is shown in dotted black. Bottom-right panel depicts the pharmacokinetically modelled estimate of IFN-concentration. For all possible doses between 0 and $20\mu g$ daily IFN, model stability for the given patient-specific parameters were determined numerically. Doses for which the healthy steady state was locally stable are shown as a green background, while doses where the full-blown leukemics steady state was found to be locally stable are shown in red. Panel (a) patient "P082" is depicted, with fit-parameters $\nu_{\rho_L} = -0.0091$, $\nu_\omega = -0.0821$, $R_{trom} = 4.1 \cdot 10^{-9}$ and $R_{leuk} = 1.5 \cdot 10^{-7}$ Panel (b) depicts patient "P198", which had fit-parameters $\nu_{\rho_L} = -0.004$, $\nu_\omega = -0.0455$, $R_{trom} = 6.5 \cdot 10^{-9}$ and $R_{leuk} = 3.1 \cdot 10^{-7}$.

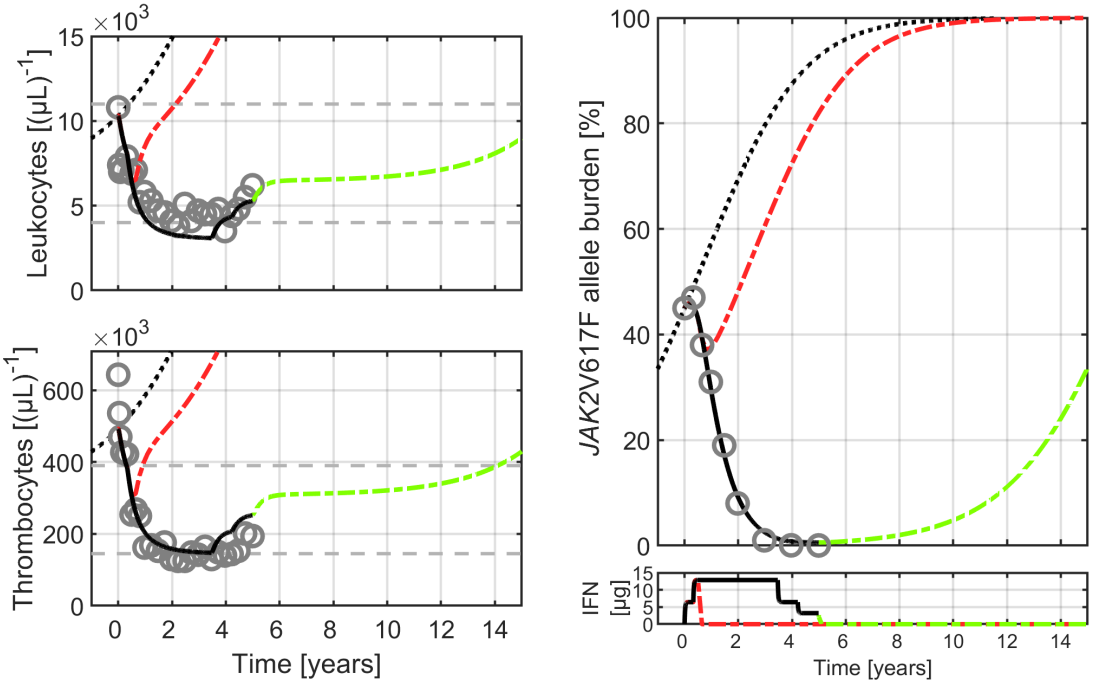


Figure 5: **Simulations of halted treatment can estimate the time to relapse.** Based on the model-fit to data for patient "P198", as shown in figure 4b, we simulated two additional scenarios: One where treatment was halted after 0.5 year, shown in dash-dotted red, and a scenario where treatment was halted at the end of the study, year 5, shown in dash-dotted green. For a full figure legend, see figure 4. The colored background of the bottom-right panel shown in figure 4 was here omitted for visual clarity.

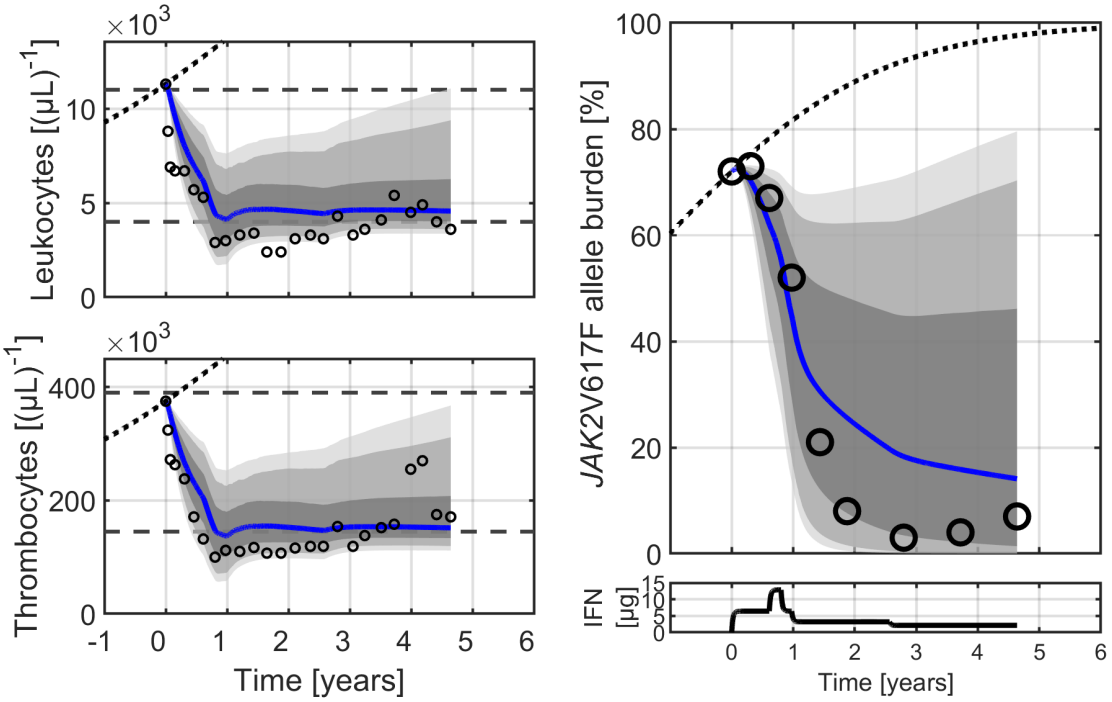


Figure 6: **Virtual patient responses based on baseline measurement and IFN dosing shows good agreement with real patient-response in some cases.** Patient data for patient "P082" is shown as black circles ◯. 1000 virtual patients were simulated and the sum of mature cells were scaled to agree with the baseline data-point for either leukocytes or thrombocytes. The blue curve shows the median response-curve. The shaded grey areas displays the distribution, with the darkest grey showing the interval from 25% to 75% of values at the given time-points, the next-darkest interval shows from 10% to 90% while the final interval from 5% to 95% of virtual patient-responses is shown in light grey. The bottom right panel displays the IFN blood-concentration used for both the real patient and the virtual patients.

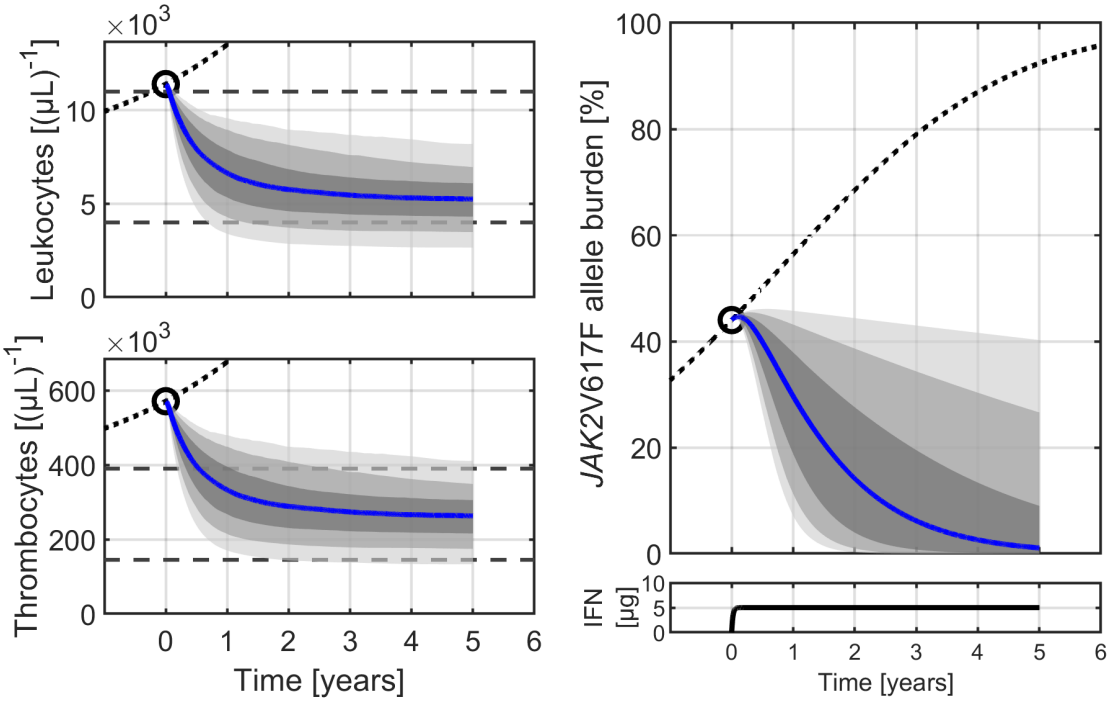


Figure 7: **Virtual patient responses based on average PV baseline measurements shows the distribution of an idealized IFN response.** Based on the average baseline values of PV patients, shown as black circles ◯, 1000 virtual patients were simulated and the sum of mature cells were scaled to agree with the baseline data-point for leukocytes and thrombocytes in the top-left and bottom-left panel respectively. The blue curve shows the median response-curve. The shaded grey areas displays the distribution, with the darkest grey showing the interval from 25% to 75% of values at the given time-points, the next-darkest interval shows from 10% to 90% while the final interval from 5% to 95% of virtual patient-responses is shown in light grey. The bottom right panel displays the IFN blood-concentration used, corresponding to a constant $5\mu g$ IFN dose.

# 5 Conclusion

A stem-cell extension of the mechanism-based Cancitis model was presented, describing simultaneously the blood-production in the human body and the behaviour of hematopoietic stem cells. Through pharmacokinetic and pharmacodynamic modelling of the effect of Interferon-alfa (IFN), the model was further extended. Considering a cohort of MPN-diagnosed patients and using patient-specific data for IFN-doses, the model reproduced both hematologic data for blood-cell counts and molecular markers describing disease burden, on the level of individual patients.

We find that normalization of cell-counts during IFN-treatment could be explained by an induced decrease in self-renewal of leukemic stem cells, and decreased proliferation of all progenitors cells. This finding agrees with and expands our previous work [21].

Apart from population-level parameters shared between patients, model-fits consisted of four fitted parameters: Two scaling-parameters of the blood-cell counts and two parameters, $\nu_{\rho_L}$ and $\nu_\omega$ The parameter $\nu_\omega$ described the number of blood-cells produced per differentiated stem cell, and was found to relate to a transient change in blood-cell counts. $\nu_{\rho_L}$ determined the proliferation of malignant stem cells, and primarily affected long-term disease burden. Furthermore, we found that the time from treatment-cessation until blood-cell counts return to a heightened value also depended on $\nu_{\rho_L}$.

Patient-specific fits were made to data for the JAK2$^{V617F}$ allele burden and the thrombocyte- and leukocyte-counts. Such simultaneous agreement with both hematologic and molecular markers are novel, and our work represent initial efforts of modelling different types of data of individual patients. The agreement between model and data demonstrates that mechanism-based mathematical modelling can accurately capture patient-behaviour, while allowing for a biological interpretation of the treatment-response. The treatment-response was quantified on a personalized level by the separate effect of $\nu_{\rho_L}$ and $\nu_\omega$, with the former parameter describing the decrease in disease burden an lengthening of the time to relapse, while the latter describes a transient decrease in blood-cell counts. In addition, our results highlight the importance of monitoring the disease burden, by demonstrating that relapse occurs earlier if treatment is ceased before the disease burden is sufficiently reduced, see figure 5.

Quantifying the two-fold effect of IFN revealed the existence of a clinical challenge. A significant response in hematologic measures, as quantified by $\nu_\omega$, suggests that high IFN-doses could lead to an excessive decrease in blood-cell-counts, which could constitute a risk for the health of the patient. However, our results simultaneously suggested that for long-term molecular response and lengthening of the time to relapse, as quantified by $\nu_{\rho_L}$, the IFN-dose must be increased. While combination therapy or novel dose-scheduling could solve this challenge, the challenge of maximizing long-term benefit while minimizing short-term risk remains. Personalized estimates of $\nu_{\rho_L}$ and $\nu_\omega$ quantifies this challenge on a personal level, identifying patients suitable for increased doses and patients that are not.

Proof-of-concept population modelling was presented. This allowed for a population-level description of the effect of IFN-treatment, and simulation of virtual patients representing the population. Comparing the distribution of 1000 virtual patients with data from a sub-cohort showed that patient-data could be predicted by the model based only on pre-treatment data and information of IFN-dose. While further validation of our approach is necessary, predicting patient-responses before treatment-initiation could be an important clinical tool. Furthermore, updating and refining predictions during subsequent clinical follow-up, could give the clinician an estimate of the patient-trajectory, guiding future clinical decisions.

In conclusion, we find that modelling the quantitative dynamics of hematologic and molecular markers on a patient-specific level during IFN-treatment is possible. In order to make accurate predictions for treatment-response based on mathematical modelling, both hematologic and molecular data are needed, highlighting the importance of obtaining molecular data in a clinical setting. Further model-validation and evaluation of the predictive power of the model is required before the model is used as a predictive clinical tool. However, we assess that personalized mathematical modelling as described here could benefit MPN-patients significantly. Furthermore, we believe that, given the similar biological structure of hematologic malignancies, such modelling could be extended to other types of blood cancers in future work, increasing the potential benefit.

# References


Andersen, M., Sajid, Z., Pedersen, R. K., Gudmand-Hoeyer, J., Ellervik, C., Skov, V., Kjær, L., Pallisgaard, N., Kruse, T. A., Thomassen, M., Troelsen, J., Hasselbalch, H. C., and Ottesen, J. T. (2017). Mathematical modelling as a proof of concept for MPNs as a human inflammation model for cancer development. *PLOS ONE*, 12(8).

Ashcroft, P., Manz, M. G., and Bonhoeffer, S. (2017). Clonal dominance and transplantation dynamics in hematopoietic stem cell compartments. *PLOS Computational Biology*, 13(10).

Becker, N. B., Günther, M., Li, C., Jolly, A., and Höfer, T. (2019). Stem cell homeostasis by integral feedback through the niche. *Journal of Theoretical Biology*, 481:100–109.

Brady, R. and Enderling, H. (2019). Mathematical Models of Cancer: When to Predict Novel Therapies, and When Not to. *Bulletin of Mathematical Biology*, 81(10):3722–3731.

Campbell, P. J. and Green, A. R. (2006). The Myeloproliferative Disorders. *New England Journal of Medicine*, 355(23):2452–2466.

Catlin, S. N., Busque, L., Gale, R. E., Guttorp, P., and Abkowitz, J. L. (2011). The replication rate of human hematopoietic stem cells in vivo. *Blood*, 117(17):4460–4466.

Clapp, G. and Levy, D. (2015). A review of mathematical models for leukemia and lymphoma. *Drug Discovery Today: Disease Models*, 16(1):1–6.

Clarke, M. A. and Fisher, J. (2020). Executable cancer models: successes and challenges. *Nature Reviews Cancer*, 20(6):343–354.

Dale, D. C. and Mackey, M. C. (2015). Understanding, Treating and Avoiding Hematological Disease: Better Medicine Through Mathematics? *Bulletin of Mathematical Biology*, 77(5):739–757.

Dingli, D. and Michor, F. (2006). Successful Therapy Must Eradicate Cancer Stem Cells. *Stem Cells*, 24(12):2603–2610.

Dingli, D. and Pacheco, J. M. (2010). Modeling the architecture and dynamics of hematopoiesis. *Wiley Interdisciplinary Reviews: Systems Biology and Medicine*, 2(2):235–244.

Dingli, D. and Pacheco, J. M. (2011). Stochastic dynamics and the evolution of mutations in stem cells. *BMC Biology*, 9(1):41.

Hasselbalch, H. C. (2013). Chronic inflammation as a promotor of mutagenesis in essential thrombocythemia, polycythemia vera and myelofibrosis. A human inflammation model for cancer development? *Leukemia Research*, 37(2):214–220.

Hasselbalch, H. C. and Bjørn, M. E. (2015). MPNs as Inflammatory Diseases: The Evidence, Consequences, and Perspectives. *Mediators of Inflammation*, 2015.

Komarova, N. L., Burger, J. A., and Wodarz, D. (2014). Evolution of ibrutinib resistance in chronic lymphocytic leukemia (CLL). *Proceedings of the National Academy of Sciences*, 111(38):13906–13911.

Komarova, N. L. and Wodarz, D. (2005). Drug resistance in cancer: Principles of emergence and prevention. *Proceedings of the National Academy of Sciences of the United States of America*, 102(27):9714–9719.

Lopes, J. V., Pacheco, J. M., and Dingli, D. (2007). Acquired hematopoietic stem-cell disorders and mammalian size. *Blood*, 110(12):4120–4122.

Mackey, M. C. (1978). Unified hypothesis for the origin of aplastic anemia and periodic hematopoiesis. *Blood*, 51(5):941–956.

Michor, F., Hughes, T. P., Iwasa, Y., Branford, S., Shah, N. P., Sawyers, C. L., and Nowak, M. A. (2005). Dynamics of chronic myeloid leukaemia. *Nature*, 435(7046):1267–1270.

Mullally, A., Bruedigam, C., Poveromo, L., Heidel, F. H., Purdon, A., Vu, T., Austin, R., Heckl, D., Breyfogle, L. J., Kuhn, C. P., Kalaitzidis, D., Armstrong, S. A., Williams, D. A., Hill, G. R., Ebert, B. L., and Lane, S. W. (2013). Depletion of Jak2V617F myeloproliferative neoplasm-propagating stem cells by interferon-$\alpha$ in a murine model of polycythemia vera. *Blood*, 121(18):3692–702.

Ottesen, J. T., Pedersen, R. K., Dam, M. J. B., Knudsen, T. A., Skov, V., Kjær, L., and Andersen, M. (2020). Mathematical Modeling of MPNs Offers Understanding and Decision Support for Personalized Treatment. *Cancers*, 12(8):2119.

Ottesen, J. T., Pedersen, R. K., Sajid, Z., Gudmand-Hoeyer, J., Bangsgaard, K. O., Skov, V., Kjær, L., Knudsen, T. A., Pallisgaard, N., Hasselbalch, H. C., and Andersen, M. (2019). Bridging blood cancers and inflammation: The reduced Cancitis model. *Journal of Theoretical Biology*, 465:90–108.

Park, D. S., Akuffo, A. A., Muench, D. E., Grimes, H. L., Epling-Burnette, P. K., Maini, P. K., Anderson, A. R. A., and Bonsall, M. B. (2019). Clonal hematopoiesis of indeterminate potential and its impact on patient trajectories after stem cell transplantation. *PLOS Computational Biology*, 15(4).

Pedersen, R. K. (2020). *Mathematical Modelling of Myeloproliferative Neoplasms and Hematopoietic Stem Cells*. PhD thesis, Roskilde University.

Pedersen, R. K., Andersen, M., Knudsen, T. A., Sajid, Z., Gudmand-Hoeyer, J., Dam, M. J. B., Skov, V., Kjær, L., Ellervik, C., Larsen, T. S., Hansen, D., Pallisgaard, N., Hasselbalch, H. C., and Ottesen, J. T. (2020). Data-driven analysis of JAK2 V617F kinetics during interferon-alpha2 treatment of patients with polycythemia vera and related neoplasms. *Cancer Medicine*, 9(6):2039–2051.

Pedersen, R. K., Andersen, M., Skov, V., Kjær, L., Hasselbalch, H. C., Ottesen, J. T., and Stiehl, T. (n.d.2). Combining stem cell mobilization with preconditioning: Insights about competition in the stem cell niche from mathematical modelling. *Submitted*.

Pedersen, R. K., Andersen, M., Stiehl, T., and Ottesen, J. T. (n.d.1). Mathematical Modelling of the Hematopoietic Stem Cell–Niche System: Clonal Dominance based on Stem Cell Fitness. *In review*.

Roeder, I., Horn, M., Glauche, I., Hochhaus, A., Mueller, M. C., and Loeffler, M. (2006). Dynamic modeling of imatinib-treated chronic myeloid leukemia: Functional insights and clinical implications. *Nature Medicine*, 12(10):1181–1184.

Saito, T., Iida, S., and Kawanishi, T. (2012). Population Pharmacokinetic-Pharmacodynamic Modeling and Simulation of Platelet Decrease Induced by Peg-interferon-alpha 2a. *Drug Metabolism and Pharmacokinetics*, 27(6):614–620.

Silver, R. T., Kiladjian, J. J., and Hasselbalch, H. C. (2013). Interferon and the treatment of polycythemia vera, essential thrombocythemia and myelofibrosis. *Expert Review of Hematology*, 6(1):49–58.

Stiehl, T., Ho, A. D., and Marciniak-Czochra, A. (2014). The impact of CD34+ cell dose on engraftment after SCTs: Personalized estimates based on mathematical modeling. *Bone Marrow Transplantation*, 49(1):30–37.

Stiehl, T. and Marciniak-Czochra, A. (2017). Stem cell self-renewal in regeneration and cancer: Insights from mathematical modeling. *Current Opinion in Systems Biology*, 5:112–120.

Stiehl, T., Wang, W., Lutz, C., and Marciniak-Czochra, A. (2020). Mathematical modeling provides evidence for niche competition in human AML and serves as a tool to improve risk stratification. *Cancer Research*, page canres.0283.2020.

Traulsen, A., Pacheco, J. M., and Dingli, D. (2010). Reproductive fitness advantage of BCR-ABL expressing leukemia cells. *Cancer Letters*, 294(1):43–48.